

# Noncovalent DNA decorations of graphene oxide and reduced graphene oxide toward water-soluble metal–carbon hybrid nanostructures *via* self-assembly†

Jinbin Liu,<sup>a</sup> Yulin Li,<sup>a</sup> Yueming Li,<sup>b</sup> Jinghong Li<sup>b</sup> and Zhaoxiang Deng<sup>\*a</sup>

Received 28th August 2009, Accepted 30th October 2009

First published as an Advance Article on the web 8th December 2009

DOI: 10.1039/b917752c

Non-covalent DNA decorations on the basal planes of graphene oxide and reduced graphene oxide nanosheets are realized. The resulting DNA–carbon bioconjugates (DNA–GO or DNA–RGO) bearing multiple thiol groups tagged on DNA strands are then employed to scaffold the two-dimensional self-assembly of gold nanoparticles (AuNPs) into metal–carbon hybrid nanostructures (namely AuNP–DNA–GO or AuNP–DNA–RGO) that may find important applications in various aspects. The resulting heteronanostructures incorporating metal nanoparticles obtained by self-assembly are highly stable and water-soluble, and can be easily isolated by gel electrophoresis to guarantee high purity. Thanks to the noncovalent features of this method, either GO or RGO do not suffer from any permanent alterations of their structures and properties. In addition, the nanoparticles still maintain their optical absorbance after being assembled, and the assembly process is highly specific. This self-assembly based method for constructing heterostructured materials is excellent at overcoming any incompatibilities between nanoparticle syntheses and the formation of hybrid structures. As a result, this strategy is easily adaptable to various other materials other than gold nanoparticles and also favors the combinatorial assembly of multiple nanophases on a single nanosheet.

## Introduction

Graphene oxide and graphene (or reduced graphene oxide) are an important class of carbon-based materials that are receiving more and more attention. These materials are very easy to produce by various well-developed procedures including those based on wet chemistry.<sup>1–16</sup> Graphene can be viewed as a good counterpart to carbon nanotubes and fullerenes but with much lower synthetic costs. The unusual thermal conductivity, mechanical stiffness, fracture strength, optical and electronic transport properties of graphene have made them promising for various applications.<sup>17–21</sup> For example, graphene or graphene-based composites have found important applications as high performance battery electrodes, gas sensors, catalysts or potential hydrogen storage matrices, mostly benefiting from their high conductivity and ultimately large surface-to-volume ratio.<sup>22–34</sup>

Nanoparticle decorated graphene platelets are emerging metal–carbon hybrid materials that are currently attracting special research efforts.<sup>35–39</sup> These nanostructures are usually produced by direct chemical nucleation of nanoparticulate phases from appropriate metal precursors (such as  $[\text{AuCl}_4]^-$ ,

$[\text{PtCl}_6]^{2-}$  and  $\text{TiCl}_3$ )<sup>35–39</sup> in the presence of solubilized graphene oxide or graphene sheets. One of these researches has shown that surfactant stabilized graphene nanosheets could be used for *in situ* growth of titania nanoparticles and the resulting hybrid structures showed high Li-ion insertion kinetics.<sup>36</sup>  $\text{TiO}_2$  decorated graphene oxide could also be prepared by dispersing graphene oxide nanosheets in a colloidal suspension of  $\text{TiO}_2$  and the resulting graphene– $\text{TiO}_2$  composites could be produced by a UV-induced reduction.<sup>39</sup>

The strong drive in making graphene and graphene oxide based nano-composites has stimulated us to develop a facile, versatile and highly controllable route to directly assemble pre-synthesized nanoparticles on the basal planes of graphene oxide (GO) and reduced graphene oxide (RGO) nanosheets in a homogeneous solution. The resulting hybrid nanostructures, which are especially beneficial for investigating any emerging and tailorable properties, could be further utilized as dissolvable “nano-surfaces” to mimic heterogeneous assembly processes that usually occur on a solid substrate.

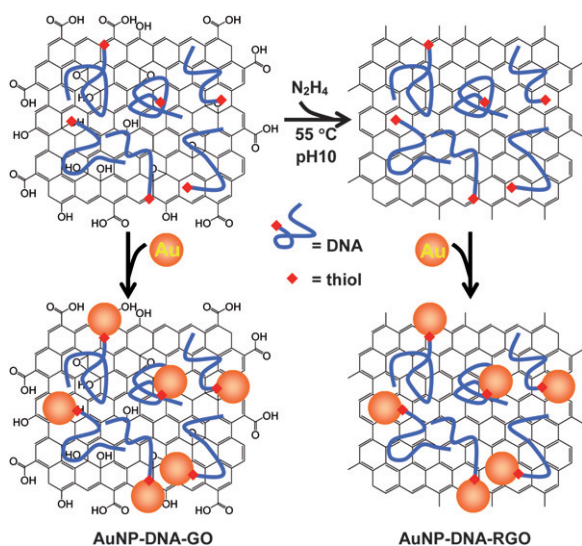
Regarding the self-assembly of pre-synthesized nanoparticles into well-defined one or two dimensional arrays and even helical nanoparticle assemblies, DNA has already played a critically important role.<sup>40–51</sup> Previous researches have shown that DNA has a strong tendency to wrap around carbon nanotubes,<sup>52,53</sup> which inspired us to attempt depositing DNA on GO and RGO surfaces in order to interface them with various nanomaterials *via* DNA assisted self-assembly. Our previous success on the assembly of gold nanoparticles (AuNPs) on single walled carbon nanotubes should be helpful for us to fulfil this goal.<sup>54,55</sup>

The strategy we developed to decorate DNA and then gold nanoparticles on the basal planes of GO and RGO is illustrated in Scheme 1. First, thiolated DNA oligos ( $\text{d}(\text{GT})_{29}\text{SH}$ ,

<sup>a</sup>CAS Key Laboratory of Soft Matter Chemistry, Department of Chemistry, University of Science and Technology of China, Hefei, Anhui, 230026, China. E-mail: zhxdeng@ustc.edu.cn; Fax: +86 551 3600950; Tel: +86 551 3600950

<sup>b</sup>Department of Chemistry, Tsinghua University, Beijing, 100084, China

† Electronic supplementary information (ESI) available: Synthetic procedure for GO; additional AFM images of the samples shown in Fig. 4; AFM images of the assembled nanoparticles on RGO by different DNA decoration strategies; pH and salt tests of GO and RGO; XPS analyses of DNA; DNA–GO and RGO samples; characterization techniques and all other experimental details. See DOI: 10.1039/b917752c



**Scheme 1** DNA coating and aqueous dispersion of graphene oxide (GO) and reduced graphene oxide (RGO), which were then used as two-dimensional bionanointerfaces for a homogeneous assembly of metal-carbon heteronanostructures.

containing 29 GT repeats) are allowed to adsorb on graphene oxide nanosheets. This is done by incubating DNA with sonication-dispersed graphene oxide sheets for a suitable time. The resulting DNA coated graphene oxide (DNA-GO) is further converted into its reduced form (DNA-RGO) by hydrazine ( $\text{N}_2\text{H}_4$ ) based chemical reduction. The DNA coated GO and RGO have a high stability in water against salt-induced coagulation, which are then separated from free DNA molecules *via* multiple centrifugation-redispersion cycles. Gold nanoparticles are then added in a large excess to a solution containing DNA-GO or DNA-RGO products. The resulting hybrid-structures between gold nanoparticles and DNA-GO or DNA-RGO are stable in water and can be separated from unbound gold nanoparticles *via* an agarose gel electrophoresis/filtration technique.

## Experimental

### Synthesis of GO

Graphene oxide (GO) was prepared according to a modified Hummer's method.<sup>4,5</sup> Synthetic details of GO are provided in the ESI.†

### Aqueous dispersion of GO

Aqueous solution of GO was obtained by dispersing 0.2 mg of as-synthesized GO in 200  $\mu\text{L}$  of doubly distilled water ( $\text{ddH}_2\text{O}$ ) under the aid of sonication for 30 min at a power of about 4 W using a UH-100A probe-type sonicator (Tianjin AutoScience Instrument Co., Ltd, China). The resulting yellow-brown suspension was then subjected to a 5 min centrifugation at 2000 g to remove undispersed particulates (in negligible amount), yielding a clear aqueous solution of GO with a concentration of about 1  $\text{mg mL}^{-1}$ .

### DNA-GO conjugates

In a typical process, 20  $\mu\text{L}$  of aqueous solution containing about 0.1  $\text{mg mL}^{-1}$  GO and 5  $\mu\text{g}$  d(GT)<sub>29</sub>SH or d(GT)<sub>29</sub> (custom-synthesized by Shanghai Sangon Biological Engineering Technology and Services Co., Ltd., China) was incubated at room temperature for 24 h, and the concentration of NaCl was slowly increased to 0.1 M during the incubation. To remove free unbound DNA, the solution was centrifuged at 16 000 g, the supernatant was discarded and the precipitated DNA-GO conjugates were then re-dispersed in 10  $\mu\text{L}$  of 0.5  $\times$  TBE buffer (Tris, 44.5 mM; boric acid, 44.5 mM; EDTA, 1 mM; pH 8.0). This precipitation-redispersion process could be repeated several times to guarantee a complete removal of free DNA.

### Preparation of RGO in the absence of DNA

RGO was prepared according to literature with slight modifications.<sup>6,56</sup> Briefly, 100  $\mu\text{L}$  of a solution containing about 0.1  $\text{mg mL}^{-1}$  GO and 0.1 M hydrazine was combined and well-mixed, and the pH of the mixture was increased to around 10 with 1.0 M NaOH. The original yellow-brown solution turned black after being heated at 55  $^\circ\text{C}$  for 6 h. The reduction process was monitored by UV absorbance spectra on a UV757CRT UV-Vis spectrophotometer (Shanghai Precision Scientific Instrument Co., Ltd., China) every 1 or 2 h. RGO samples for X-ray photoelectron spectroscopy (XPS) characterizations were precipitated by high speed centrifugation (16 000 g, 30 min), and the resulting black solids were collected and further washed with copious amount of  $\text{ddH}_2\text{O}$ .

### Hydrazine reduction of GO in the present of DNA

Similar to the preparation of RGO in the absence of DNA as described in the above procedure, 20  $\mu\text{L}$  of a solution containing 0.1  $\text{mg mL}^{-1}$  GO, 5  $\mu\text{g}$  DNA (d(GT)<sub>29</sub>SH, d(GT)<sub>29</sub>, d(GA)<sub>29</sub>SH or d(GA)<sub>29</sub>), 5 mM EDTA, 0.1 M hydrazine and 0.05 M NaCl was vortex-stirred several times. The pH of the solution was adjusted to around 10 with 1.0 M NaOH. The yellow-brown suspension of GO turned black after it was heated for 6 h at 55  $^\circ\text{C}$ . Typically, after the reduction reaction, a further incubation of the sample at room temperature for 18 h was allowed before the removal of free unbound DNA by high speed centrifugation. NaCl concentration was further increased to 0.1 M during this prolonged incubation.

### Hydrazine reduction of GO followed by addition of DNA

In order to avoid DNA damages due to the treatment in hydrazine at elevated temperature (55  $^\circ\text{C}$ ), the reduction of GO was performed before the addition of DNA. Keeping the sample pH around 10 was able to maintain the freshly reduced RGO product well-dispersed in the absence of DNA. A 2.5  $\mu\text{L}$  aliquot of 5  $\mu\text{g}$  DNA (d(GT)<sub>29</sub>SH or d(GT)<sub>29</sub>), supplemented with 0.5  $\mu\text{L}$  of 0.2 M EDTA, was then added to 20  $\mu\text{L}$  (originally containing 0.1  $\text{mg mL}^{-1}$  GO) freshly produced RGO solution. Decoration of RGO by DNA was allowed to proceed during a 24 h incubation with the concentration of NaCl gradually increased to 0.1 M. To remove free DNA and hydrazine, the resulting RGO solution

was centrifuged at 16 000 g, with the supernatant discarded and the DNA–RGO conjugates re-dispersed in 10  $\mu$ L 0.5  $\times$  TBE.

### Formations of AuNP–DNA–GO and AuNP–DNA–RGO

AuNP–DNA–GO (or RGO) was prepared by incubating DNA–GO (or DNA–RGO) with an excess amount of phosphine-protected gold nanoparticles (6 nm diameter, please refer to our earlier publications<sup>54,57</sup> for synthesis and characterization details) in 0.5  $\times$  TBE buffer supplemented with 0.1 M NaCl for 12 h. To remove unbound gold nanoparticles and isolate the AuNP–DNA–GO (or RGO) assemblies, the reaction mixture was loaded on a 2% agarose gel and run in 0.5  $\times$  TBE at 10 V  $\text{cm}^{-1}$  for 30 min. The assembled AuNP–DNA–GO (or AuNP–DNA–RGO) conjugates could not migrate into the gel, and thus could be easily collected by rinsing the corresponding gel wells with 20  $\mu$ L running buffer. The recovered assemblies were directly examined by atomic force microscopy (AFM) and UV-Vis absorbance spectroscopy.

### Results and discussion

The interactions between DNA and RGO could be attributed to the strong  $\pi$ – $\pi$  stacking force, which is similar to the case of DNA wrapping on carbon nanotubes.<sup>52,53</sup> Theoretical calculations have been previously carried out to provide more details about the interactions between DNA bases and graphene or

carbon nanotube surfaces.<sup>58,59</sup> On the surface of GO, graphene-like local conjugated domains should be existent, which could be responsible for DNA adsorption. In addition, hydrogen bondings between DNA and some oxygen-containing groups on GO might be another driving force for DNA deposition on GO nanosheets.

We monitored the chemical reduction process of GO by UV absorbance spectroscopy. As can be seen from Fig. 1a, an absorbance at 230 nm (typical for GO) gradually shifted to around 266 nm during the reduction process, consistent with literature reports.<sup>56</sup> The overall increase of the absorbance spectra with time further suggested a successful recovery of electronic conjugations within the RGO nanosheets during the hydrazine reduction. X-Ray photoelectron spectroscopy (XPS) was employed to characterize the samples before and after the chemical reductions by hydrazine. We purposely omitted DNA during the preparation of RGO samples for XPS analyses in order to avoid interfering XPS signals from DNA. High resolution XPS scans in Fig. 1b show an obvious diminishing of C=O and C–O contents in the RGO sample, which evidenced a successful conversion from GO to RGO.

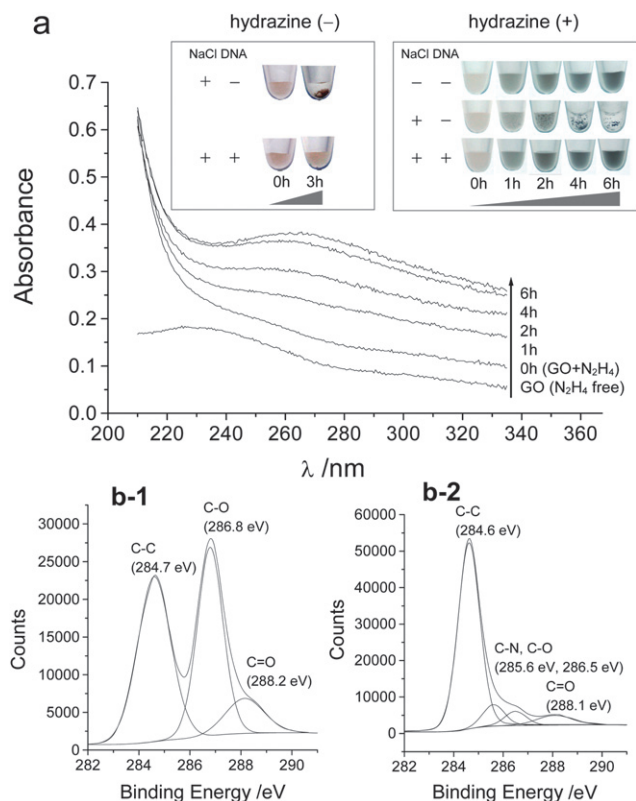


**Fig. 1** Reduction of GO by hydrazine. (a) Monitoring the reduction process by UV absorbance in the absence of DNA. (b) C1s XPS spectra of GO (b-1) and RGO (b-2) samples in the absence of DNA. Inset in (a): salt resistivity tests of GO (left) and RGO (right) in the presence or absence of DNA.

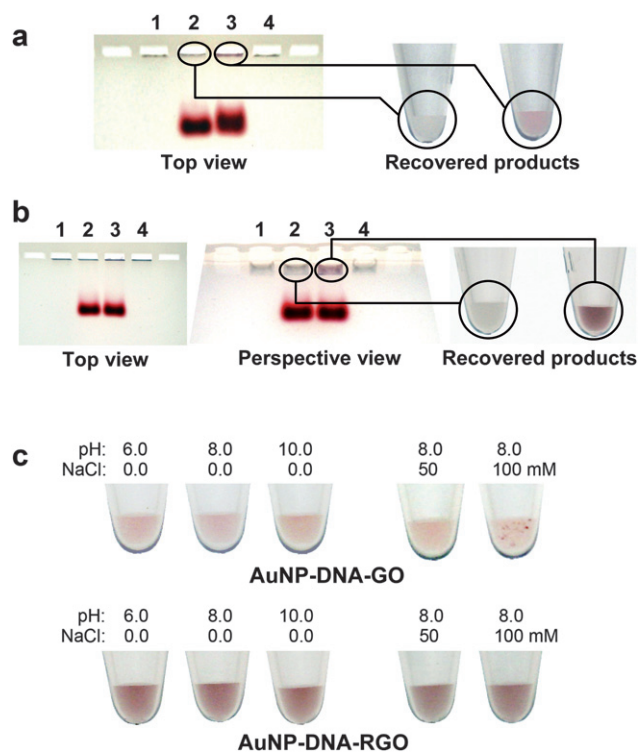


**Fig. 2** Electrophoretic isolations and stability tests of the assembled hybrid nanostructures formed between AuNPs and GO or RGO. (a, b) AuNP–DNA–GO (a) and AuNP–DNA–RGO (b) conjugates obtained by DNA assisted assembly. Lanes 1–4 in the agarose gels represent d(GT)<sub>29</sub>–GO (or RGO), d(GT)<sub>29</sub>–GO (or RGO) + AuNPs, d(GT)<sub>29</sub>SH–GO (or RGO) + AuNPs, and d(GT)<sub>29</sub>SH–GO (or RGO), respectively. (c) NaCl and pH stability tests of the hybrid nanostructures indicating that the products were stable in aqueous solutions. The AuNP–DNA–GO sample was slightly destabilized in the presence of 0.1 M NaCl (some red-colored macro-aggregates were visible). During stability investigations, brief centrifugations at 2000 g for 30 s accelerated the formation of precipitates in destabilized samples for easy observation.

Successful DNA decorations of GO and RGO could be preliminarily judged by NaCl or pH stability tests of the resulting colloidal dispersions against agglomerations. As shown in Fig. 1a, the addition of hydrazine to a solution of GO at 55 °C immediately triggered a chemical reduction reaction, as could be judged from the darkening of solutions. As a control experiment, omitting DNA from the reaction caused the reduced product to precipitate after an addition of 0.05 M NaCl, which could be rationalized by a gradual loss of hydrophilic oxygen-containing groups from a GO nanosheet during the reduction process. Although the RGO product had some stability at pH 10 in the absence of DNA due to the existence of some carboxylic residues, a further pH switching to 6.0 completely destabilized the RGO suspension (Fig. S1†). Similarly, in the case of GO, the addition of DNA significantly increased its stability against the presence of 0.1 M NaCl (Fig. 1a, left inset).

In the following experiments, GO and RGO nanosheets were employed to scaffold the two-dimensional assembly of gold nanoparticles. This process started with the addition of excess amount of gold nanoparticles to a solution of GO or RGO that had been coated with thiol-tagged d(GT)<sub>29</sub> oligos. The binding of gold nanoparticles to RGO or GO was allowed to take place during an overnight incubation at room temperature (22 °C). The products were then subjected to electrophoretic separation in an agarose gel. Gel images in Fig. 2 clearly showed the reddish assemblies retarded in gel loading wells due to their relatively bulky sizes. Unbound gold nanoparticles, which were added in

excess to minimize nanoparticle-induced aggregations of GO or RGO, easily penetrated into the gel matrices and were readily separated from the assembled products.

The products deposited on the accumulation walls (facing the negative electrode) inside the gel wells could be easily recovered by rinsing the wells with small volumes of buffer solutions. The gel purified assemblies had a very obvious reddish color, characteristic of the plasmonic absorbance of gold nanoparticles (see microtubes in Fig. 2 and UV-Vis spectra in Fig. 3), in sharp contrast to the control samples in which thiol-free DNA were

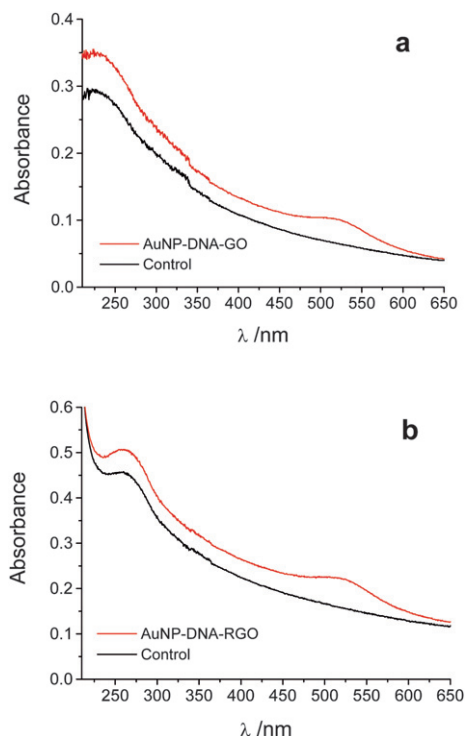


**Fig. 3** UV-Vis absorbance curves of the hybrid nanostructures formed between gold nanoparticles and graphene oxide (a) or reduced graphene oxide (b). The products were purified through agarose gel filtration and the absorbance peaks around 520 nm were well consistent with the surface plasmon resonance of 6 nm gold nanoparticles. Control GO and RGO samples dispersed using thiol-free DNA were not able to incorporate gold nanoparticles.

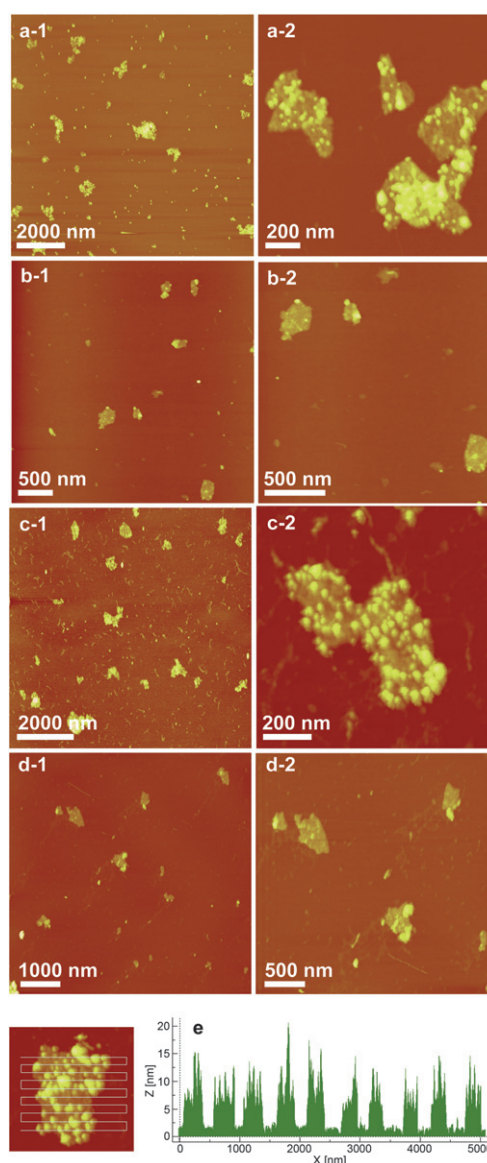


**Fig. 4** AFM images of DNA decorated (a, b) GO and (c, d, e) RGO nanosheets after being interacted with 6 nm gold nanoparticles. (a, c, e) d(GT)<sub>29</sub>SH decorated GO (a) and RGO (c, e) after the assembly of gold nanoparticles; (b, d) control experiments showing that d(GT)<sub>29</sub> (no thiol tag) decorated GO (b) and RGO (d) were not able to attach gold nanoparticles; (e) height profile analysis of a RGO nanosheet decorated with 6 nm gold nanoparticles, based on which the height of RGO was found to be about 4 nm, and the diameter (measured as height in AFM) of decorated gold nanoparticles was 4–9 nm (large particle aggregates were excluded). Additional AFM images are given in Fig. S4–S7.†

used to decorate the nanosheets (lanes 2 in Fig. 2a, b). These results provided a strong evidence for the successful conjugations between nanoparticles and carbon nanosheets. In addition, the absorbance data in Fig. 3 revealed that the gold nanoparticles were able to preserve their optical properties even after being immobilized on the GO or RGO nanosheets, which is another important feature of this assembly-based process. For the previously reported *in situ* reduction based nucleation processes, it would be difficult (if not impossible) to prepare metal nanoparticle decorated GO nanosheets since the required chemical reduction processes would convert (at least partially) GO to RGO. The as-obtained hybrid structures between gold nanoparticles and GO/RGO were highly stable (see Fig. 2c) at acidic and basic pHs, or in the presence of 0.05–0.1 M NaCl, which will be attractive for various downstream applications such as microcontact printing or ink-jet based nanofabrications. The insulator property and low-cost synthesis of GO make the corresponding hybrid lamellar structures bearing metal nanoparticles ideal for making conductivity based sensors if a further electroless metal deposition seeded by the assembled metal particles was performed to generate conductivity signals.

Because the absorbance of DNA could not be easily resolved from the UV spectra of DNA–GO and DNA–RGO due to the strong absorbance background from GO and RGO (Fig. 3 and S15†), XPS was further employed as a better characterization technique for these samples to provide direct evidences for the existence of DNA by monitoring the phosphorus and nitrogen contents coming from the phosphate backbones and DNA bases (Fig. S16–18†). The XPS evidences, the stability tests against salt and pH induced agglomerations, along with the highly specific decorations of gold nanoparticles that reflected the existence of abundant amount of thiol groups on the GO and RGO surfaces, all unambiguously revealed the successful DNA decorations of GO and RGO nanosheets.

We further relied on atomic force microscopy (AFM) to directly look at the assembled structures. The samples were deposited on  $Mg^{2+}$  treated freshly cleaved mica surfaces and then subjected to AFM imaging. Fig. 4 provides an array of randomly chosen AFM images for different samples, from which gold nanoparticles decorated on graphene oxide and reduced graphene oxide nanosheets were clearly visible (also see Fig. S4 and S6†). Section analysis of an AuNP–DNA–RGO assembly revealed that the RGO nanosheet had a height around 4 nm and the surface-adsorbed particles had typical heights of 4–9 nm (close to the 6 nm average diameter of as-prepared individual AuNPs). DNA-free RGO nanosheets were found to have a typical height of 1.5 nm (Fig. S2†). Considering there were

unstructured DNA coils (Scheme 1) adsorbed on both sides of a nanosheet, this height increase of 2.5 nm for DNA coated RGO was reasonable. Besides, the measured thicknesses of DNA-free RGO and GO (see Fig. S2–S3†) probably meant that more than a single atomic layer was included in some nanosheets.

To exclude the existence of non-specific interactions between AuNPs and DNA–RGO/GO nanosheets, control experiments were carried out using GO and RGO samples decorated with thiol-free DNA as assembly templates. AFM images in Fig. 4b, d clearly show that the GO and RGO nanosheets decorated with thiol-free DNA were almost free of adsorbed nanoparticles (Fig. S5 and S7†). In combination with the gel evidences in Fig. 2, the high specificity of this assembly process was verified. In addition, no significant detachments of the assembled nanoparticles were observed during AFM imagings even after multiple sample washings, suggesting that the AuNPs on nanosheets were quite stable.

As the hydrazine treatment at elevated temperatures might be dangerous to DNA sequences containing thymine or cytosine bases due to a well-known hydrazinolysis process (the basis of Maxam–Gilbert DNA sequencing).<sup>60,61</sup> Although this process did not show any obvious influence on the assembly of gold nanoparticles (AuNPs) on RGO, it still appeared necessary to check if this damage did happen under our experimental conditions. We thus sequentially incubated  $d(GT)_{29}$  with hydrazine and then piperidine (responsible for a strand scission process) and used denaturing polyacrylamide gel electrophoresis (PAGE) to observe DNA degradations. The gel data in Fig. 5a did show some degradations (but still to an acceptable extent) of  $d(GT)_{29}$ . As a comparison, we tested a  $d(GA)_{29}$  sequence by the same treatments since this sequence was free of thymine and cytosine bases and would be more resistant to the hydrazinolysis reaction. Fig. 5b shows that the damage to  $d(GA)_{29}$  was almost negligible. However, in the case of attaching AuNPs (Fig. S8†), no obvious advantages of  $d(GA)_{29}$  over  $d(GT)_{29}$  were observed. One possible reason could be that our assembly process did not require exposing DNA to piperidine, which meant the continuity of the chemically altered DNA strands was still maintained and, therefore, thiol tags were still there.<sup>60,61</sup> The interaction between the partially damaged  $d(GT)_{29}$  sequence and RGO or GO was strong enough to secure an efficient assembly process.

If the DNA bases must be kept intact for some hybridization-based experiments that are currently under investigation,<sup>55</sup> a sonication-assisted DNA dispersion of already reduced graphene products (precipitated), similar to the case of carbon nanotubes,<sup>52–55</sup> could be attempted to disperse RGO (see Fig. S9† for results). Besides, we also tried to add DNA after the

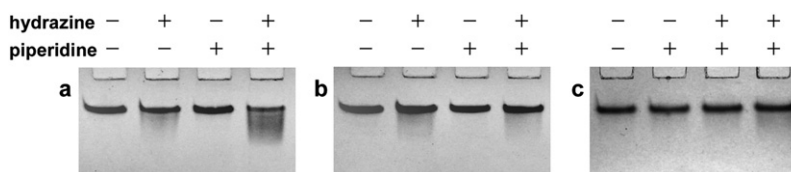


**Fig. 5** Denaturing PAGE gels showing different degradation behaviors of (a, c)  $d(GT)_{29}$  and (b)  $d(GA)_{29}$  sequences after been treated with hydrazine and piperidine. Note that the last two lanes in (c) corresponded to a hydrazine treatment at room temperature for 4 and 24 h, respectively. In other cases, the interactions between hydrazine and DNA were at 55 °C for 6 h. See ESI for experimental details.† (a, b) DNA strands were present during hydrazine reductions; (c) DNA was introduced after the hydrazine-based reduction had been finished.

reduction of GO had been finished and the samples being cooled down to room temperature (DNA cleavage was negligible under this condition, see Fig. 5c). At pH 10, we could keep the RGO product well-dispersed before the DNA sequences were introduced (see Fig. 1a, right inset). A further incubation of RGO with DNA over a period of 24 h at room temperature was more than enough to obtain DNA coated RGO nanosheets for the assembly of gold nanoparticles (see Fig. S10–14† for the assembly results). This method showed a success in greatly alleviating the damages to DNA, which might be an ultimate solution to the DNA degradation problem either due to hydrazinolysis or sonication induced mechanical cleavage.

The procedures adopted in this work to obtain DNA coated GO and RGO were much simpler and more efficient than the methods employed to produce DNA wrapped carbon nanotubes, as no sonication was needed to facilitate DNA adsorption. Due to the bulkier size of graphene nanosheets compared to single walled carbon nanotubes, isolations of resulting metal–carbon assemblies by gel electrophoresis were much easier. We should also note here that all the AuNP–DNA–GO/RGO products were homogeneously dissolved in an aqueous solution (Fig. 2), which was especially favorable for their various future applications. As a contrast, other methods including chemical depositions of nanoparticles on RGO often resulted in precipitates of the hybrid nanostructures.

## Conclusions

In conclusion, we have successfully demonstrated that DNA decorated graphene oxide and reduced graphene oxide were especially suitable for the organization of gold nanoparticles into two-dimensional hybrid nanoarrays. The DNA directed assembly of metal–carbon heteronanostructures represents a general, easy, highly specific, non-destructive and environmental-friendly process for nano-constructions. The use of pre-synthesized nanoparticles for a direct assembly of metal–carbon hybrid structures eliminated any possible incompatibilities between particle synthesis and assembly. Therefore, in sharp contrast to the *in situ* growth strategies, our method will have an easy and direct stoichiometric control between nanoparticles and graphene nanosheets and, more importantly, allows the assembly of different functional nano-objects on a single nanosheet toward novel composite structures.

Foreseeable applications of these structures include catalysis, magnetism, battery materials, optoelectronics, field effect devices and biodetection platforms. The good water solubility of the resulting nanostructures also makes them compatible with ink-jet or micro-contact printing based device fabrications. Some applications of DNA decorated GO and RGO have been demonstrated.<sup>31,62</sup> Our work will be helpful for any experimental attempts toward synthesizing and harnessing the properties of graphene oxide or reduced graphene oxide based hybrid materials. In addition, our work also provides a very convenient way to make metal–GO hybrids, which are difficult to obtain by *in situ* chemical reduction based strategies. Because graphene oxide is an insulating material, it is possible to develop conductivity based sensors with the attached gold nanoparticles as catalytic nucleation centers for further metal deposition to achieve conductivity signals. Since pristine graphene has a basal

surface very similar to highly oriented pyrolytic graphite (HOPG), we expect to use small molecules to decorate the graphene surface toward an ordered array of nanoparticle anchoring points. The very low production cost of graphene related materials, which are also free of catalyst residues, will make them very attractive for the above-mentioned applications.

## Acknowledgements

This work was supported by National Natural Science Foundation of China (Grant No. 20605019, 20873134), the University of Science and Technology of China (a start-up fund), Chinese Academy of Sciences (a Bairen professorship supporting fund), and PCSIRT (IRT0756). The authors are grateful to Prof. W. Huang's group for their help in XPS peak fittings.

## References

- 1 S. Park and R. S. Ruoff, *Nat. Nanotechnol.*, 2009, **4**, 217.
- 2 B. C. Brodie, *Ann. Chim. Phys.*, 1860, **59**, 466.
- 3 L. Staudenmaier, *Ber. Dtsch. Chem. Ges.*, 1898, **31**, 1481.
- 4 W. S. Hummers and R. E. Offeman, *J. Am. Chem. Soc.*, 1958, **80**, 1339.
- 5 N. I. Kovtyukhova, P. J. Ollivier, B. R. Martin, T. E. Mallouk, S. A. Chizhik, E. V. Buzaneva and A. D. Gorchinskiy, *Chem. Mater.*, 1999, **11**, 771.
- 6 S. J. Park, J. H. An, R. D. Piner, I. H. Jung, D. X. Yang, A. Velamakanni, S. B. T. Nguyen and R. S. Ruoff, *Chem. Mater.*, 2008, **20**, 6592.
- 7 S. Stankovich, D. A. Dikin, R. D. Piner, K. A. Kohlhaas, A. Kleinhammes, Y. Y. Jia, Y. Wu, S. T. Nguyen and R. S. Ruoff, *Carbon*, 2007, **45**, 1558.
- 8 J. R. Lomeda, C. D. Doyle, D. V. Kosynkin, W. F. Hwang and J. M. Tour, *J. Am. Chem. Soc.*, 2008, **130**, 16201.
- 9 V. C. Tung, M. J. Allen, Y. Yang and R. B. Kaner, *Nat. Nanotechnol.*, 2009, **4**, 25.
- 10 G. X. Wang, J. Yang, J. Park, X. L. Gou, B. Wang, H. Liu and J. Yao, *J. Phys. Chem. C*, 2008, **112**, 8192.
- 11 H. C. Schniepp, J. L. Li, M. J. McAllister, H. Sai, M. Herrera-Alonso, D. H. Adamson, R. K. Prud'homme, R. Car, D. A. Saville and I. A. Aksay, *J. Phys. Chem. B*, 2006, **110**, 8535.
- 12 M. J. McAllister, J. L. Li, D. H. Adamson, H. C. Schniepp, A. A. Abdala, J. Liu, M. Herrera-Alonso, D. L. Milius, R. Car, R. K. Prud'homme and I. A. Aksay, *Chem. Mater.*, 2007, **19**, 4396.
- 13 Y. C. Si and E. T. Samulski, *Nano Lett.*, 2008, **8**, 1679.
- 14 L. Y. Jiao, L. Zhang, X. R. Wang, G. Diankov and H. J. Dai, *Nature*, 2009, **458**, 877.
- 15 D. V. Kosynkin, A. L. Higginbotham, A. Sinitskii, J. R. Lomeda, A. Dimiev, B. K. Price and J. M. Tour, *Nature*, 2009, **458**, 872.
- 16 X. L. Li, X. R. Wang, L. Zhang, S. W. Lee and H. J. Dai, *Science*, 2008, **319**, 1229.
- 17 A. K. Geim and K. S. Novoselov, *Nat. Mater.*, 2007, **6**, 183.
- 18 A. A. Balandin, S. Ghosh, W. Z. Bao, I. Calizo, D. Teweldebrhan, F. Miao and C. N. Lau, *Nano Lett.*, 2008, **8**, 902.
- 19 K. I. Bolotin, K. J. Sikes, Z. Jiang, M. Klima, G. Fudenberg, J. Hone, P. Kim and H. L. Stormer, *Solid State Commun.*, 2008, **146**, 351.
- 20 M. D. Stoller, S. Park, Y. Zhu, J. An and R. S. Ruoff, *Nano Lett.*, 2008, **8**, 3498.
- 21 Y. Zhang, Y. W. Tan, H. L. Stormer and P. Kim, *Nature*, 2005, **438**, 201.
- 22 A. Peigney, C. Laurent, E. Flahaut, R. R. Bacsá and A. Rousset, *Carbon*, 2001, **39**, 507.
- 23 E. Yoo, J. Kim, E. Hosono, H. S. Zhou, T. Kudo and I. Honma, *Nano Lett.*, 2008, **8**, 2277.
- 24 S. M. Paek, E. J. Yoo and I. Honma, *Nano Lett.*, 2009, **9**, 72.
- 25 S. Patchkovskii, J. S. Tse, S. N. Yurchenko, L. Zhechkov, T. Heine and G. Seifert, *Proc. Natl. Acad. Sci. U. S. A.*, 2005, **102**, 10439.
- 26 C. Xu, X. Wang and J. W. Zhu, *J. Phys. Chem. C*, 2008, **112**, 19841.
- 27 R. Kou, Y. Y. Shao, D. H. Wang, M. H. Engelhard, J. H. Kwak, J. Wang, V. V. Viswanathan, C. M. Wang, Y. H. Lin, Y. Wang, I. A. Aksay and J. Liu, *Electrochem. Commun.*, 2009, **11**, 954.

- 28 F. Schedin, A. K. Geim, S. V. Morozov, E. W. Hill, P. Blake, M. I. Katsnelson and K. S. Novoselov, *Nat. Mater.*, 2007, **6**, 652.
- 29 Q. Liu, Z. Liu, X. Zhang, N. Zhang, L. Yang, S. Yin and Y. Chen, *Appl. Phys. Lett.*, 2008, **92**, 223303.
- 30 X. Wang, *Angew. Chem., Int. Ed.*, 2008, **47**, 2990.
- 31 N. Mohanty and V. Berry, *Nano Lett.*, 2008, **8**, 4469.
- 32 V. Grigorieva and A. A. Firsov, *Science*, 2004, **306**, 666.
- 33 S. Stankovich, D. A. Dikin, G. H. B. Dommett, K. M. Kohlhaas, E. J. Zimney, E. A. Stach, R. D. Piner, S. T. Nguyen and R. S. Ruoff, *Nature*, 2006, **442**, 282.
- 34 T. Ramanathan, A. A. Abdala, S. Stankovich, D. A. Dikin, M. Herrera-Alonso, R. D. Piner, D. H. Adamson, H. C. Schniepp, X. Chen, R. S. Ruoff, S. T. Nguyen, I. A. Aksay, R. K. Prud'homme and L. C. Brinson, *Nat. Nanotechnol.*, 2008, **3**, 327.
- 35 R. Muszynski, B. Seger and P. V. Kamat, *J. Phys. Chem. C*, 2008, **112**, 5263.
- 36 D. H. Wang, D. Choi, J. Li, Z. G. Yang, Z. M. Nie, R. Kou, D. H. Hu, C. M. Wang, L. V. Saraf, J. G. Zhang, L. A. Aksay and J. Liu, *ACS Nano*, 2009, **3**, 907.
- 37 Y. M. Li, L. H. Tang and J. H. Li, *Electrochem. Commun.*, 2009, **11**, 846.
- 38 B. S. Kong, J. X. Geng and H. T. Jung, *Chem. Commun.*, 2009, 2174.
- 39 G. Williams, B. Seger and P. V. Kamat, *ACS Nano*, 2008, **2**, 1487.
- 40 N. C. Seeman, *Nature*, 2003, **421**, 427.
- 41 C. J. Loweth, W. B. Caldwell, X. G. Peng, A. P. Alivisatos and P. G. Schultz, *Angew. Chem., Int. Ed.*, 1999, **38**, 1808.
- 42 C. M. Niemeyer, W. Bürger and J. Peplies, *Angew. Chem., Int. Ed.*, 1998, **37**, 2265.
- 43 Z. X. Deng, Y. Tian, S. H. Lee and C. D. Mao, *Angew. Chem., Int. Ed.*, 2005, **44**, 3582.
- 44 J. D. Le, Y. Pinto, N. C. Seeman, K. Musier-Forsyth, T. A. Taton and R. A. Kiehl, *Nano Lett.*, 2004, **4**, 2343.
- 45 J. W. Zheng, P. E. Constantinou, C. Micheel, A. P. Alivisatos, R. A. Kiehl and N. C. Seeman, *Nano Lett.*, 2006, **6**, 1502.
- 46 J. Sharma, R. Chhabra, Y. Liu, Y. G. Ke and H. Yan, *Angew. Chem., Int. Ed.*, 2006, **45**, 730.
- 47 H. Yan, S. H. Park, G. Finkelstein, J. H. Reif and T. H. LaBean, *Science*, 2003, **301**, 1882.
- 48 S. Y. Park, A. K. R. Lytton-Jean, B. Lee, S. Weigand, G. C. Schatz and C. A. Mirkin, *Nature*, 2008, **451**, 553.
- 49 D. Nykypanchuk, M. M. Maye, D. van der Lelie and O. Gang, *Nature*, 2008, **451**, 549.
- 50 J. Sharma, R. Chhabra, A. Cheng, J. Brownell, Y. Liu and H. Yan, *Science*, 2009, **323**, 112.
- 51 M. M. Maye, D. Nykypanchuk, M. Cuisinier, D. van der Lelie and O. Gang, *Nat. Mater.*, 2009, **8**, 388.
- 52 M. Zheng, A. Jagota, M. S. Strano, A. P. Santos, P. Barone, S. G. Chou, B. A. Diner, M. S. Dresselhaus, R. S. McLean, G. B. Onoa, G. G. Samsonidze, E. D. Semke, M. Usrey and D. J. Walls, *Science*, 2003, **302**, 1545.
- 53 M. Zheng, A. Jagota, E. D. Semke, B. A. Diner, R. S. Mclean, S. R. Lustig, R. E. Richardson and N. G. Tassi, *Nat. Mater.*, 2003, **2**, 338.
- 54 X. G. Han, Y. L. Li and Z. X. Deng, *Adv. Mater.*, 2007, **19**, 1518.
- 55 Y. L. Li, X. G. Han and Z. X. Deng, *Angew. Chem., Int. Ed.*, 2007, **46**, 7481.
- 56 D. Li, M. B. Muller, S. Gilje, R. B. Kaner and G. G. Wallace, *Nat. Nanotechnol.*, 2008, **3**, 101.
- 57 X. G. Han, Y. L. Li, S. G. Wu and Z. X. Deng, *Small*, 2008, **4**, 326.
- 58 S. Gowtham, R. H. Scheicher, R. Ahuja, R. Pandey and S. P. Karna, *Phys. Rev. B: Condens. Matter Mater. Phys.*, 2007, **76**, 033401.
- 59 A. Das, A. K. Sood, P. K. Maiti, M. Das, R. Varadarajan and C. N. R. Rao, *Chem. Phys. Lett.*, 2008, **453**, 266.
- 60 A. M. Maxam and W. Gilbert, *Proc. Natl. Acad. Sci. U. S. A.*, 1977, **74**, 560.
- 61 A. R. Cashmore and G. B. Petersen, *Nucleic Acids Res.*, 1978, **5**, 2485.
- 62 During the preparation of this paper, we noted that two other groups are using DNA to disperse graphene oxide and graphene nanosheets to build fluorescent sensors and free standing graphene membrane. See: (a) A. J. Patil, J. L. Vickery, T. B. Scott and S. Mann, *Adv. Mater.*, 2009, **21**, 3159; (b) C. H. Lu, H. H. Yang, C. L. Zhu, X. Chen and G. N. Chen, *Angew. Chem., Int. Ed.*, 2009, **48**, 4785.